Dip moveout and Stolt migration using the singular value decomposition

Stewart A. Levin

Fabio Rocca

ABSTRACT

Phase shift migration, after simple modifications, produces accurate images of synthetic aperture array radar (SAR) signals. Approximating the matrix of phase shifts with the largest term of its singular value decomposition (SVD) yields an analog of Stolt migration. This SVD-Stolt migration permits rapid computation, often without undue loss of accuracy. In this paper, we apply the SVD method to seismic processing by developing a rapid method for dip moveout (DMO) in constant velocity. We also use SVD to study extensions to Stolt migration when velocity is no longer constant with depth. Lastly, we suggest several further applications and directions for future research.

INTRODUCTION

Migration is pure-phase focusing. Image samples are generated by aligning and summing hyperbolic incoming arrivals. This alignment may be done by means such as normal-moveout correction, finite-difference wave extrapolation, or frequency-wavenumber phase shifting. When computationally feasible, the F-K phase-shift method is preferable because it gives very accurate alignment.

In synthetic array radar, the arrivals to be focused aren't hyperbolic, but their shapes and corresponding phase shifts are easily determined analytically or by ray-tracing. For real-time satellite radar imagery, phase shifts can be precomputed to save time. However, satellite radar collects samples very rapidly and to even apply the phase shifts at compatible rates requires hundreds of gigaflops of specialized computing power, a prohibitively expensive proposition. Fast, approximate methods must be used. One of these is the SVD-Stolt method.

SVD-STOLT METHOD

The SVD-Stolt method, like Stolt migration, uses a change of variable to convert a phase-shift integral into a Fourier transform. To better understand this, let us represent a generic phase shift focusing scheme as a phase-shift integral

$$M(\tau;k) \;=\; \int e^{\,i\,\phi(\tau,\omega;k)}\, P(\,\omega;k\,)\; d\,\omega \qquad , \tag{1}$$

where the image M is produced by phase-shifting the input data P with suitable phase shifts ϕ. For each fixed spatial wavenumber k, approximate ϕ with a separable product of two functions $u(\tau)$ and $v(\omega)$. Substituting this into equation (1), we get

$$M(\tau,k) \;=\; \int e^{\,iu(\tau)v(\omega)}\, P(\,\omega,k\,)\; d\,\omega \qquad . \tag{2}$$

If we now change variables in the integration from ω to v, we obtain the three-step migration process

$$\begin{aligned} Q(v\,,k) &= P(\,\omega(v\,),k\,)\; d\,\omega/dv \\ N(u\,,k) &= \int e^{\,iuv}\, Q(v\,,k\,)dv \\ M(\,\tau,k\,) &= N(u(\tau),k\,) \qquad , \end{aligned} \tag{3}$$

a Stolt-like mapping of the ω–k domain followed by an inverse Fourier transform, and a second Stolt-like mapping of the τ–k plane.

For constant velocity migration, the mapping functions

$$\begin{aligned} u(\tau) &= \tau \qquad \text{and} \\ v(\omega) &= \operatorname{sgn}\omega \left(\omega^2 - v^2k^2\right)^{1/2} \end{aligned} \tag{4}$$

produce an exact fit to ϕ, yielding ordinary Stolt migration. This is, of course, an exceptional case. For a general phase shift function ϕ, we have no guarantee that any separable product $u(\tau)v(\omega)$ will be a good approximation. When one exists, it further is unlikely to have a useful analytic form. For this reason, further discussion is confined to the discrete version here.

After the axes are discretized, the phase shifts ϕ may be represented as an $m \times n$ matrix. Any separable approximation can be written as a rank-one product $u\; v^T$ for suitable vectors u and v of size m and n respectively. A classic least-squares result (see Levin 1985a) is that optimal choices for u and v are given by the left and right singular vectors corresponding to the largest singular value in the singular value decomposition (SVD) of ϕ. Here, the remaining singular vectors are not of particular interest. The sum of squares of the other singular values is, however, a measure of how close the separable approximation is to the original phase-shift matrix. When the sum is small compared to the square of the largest singular value, the fit is good and we can expect an accurate migration.

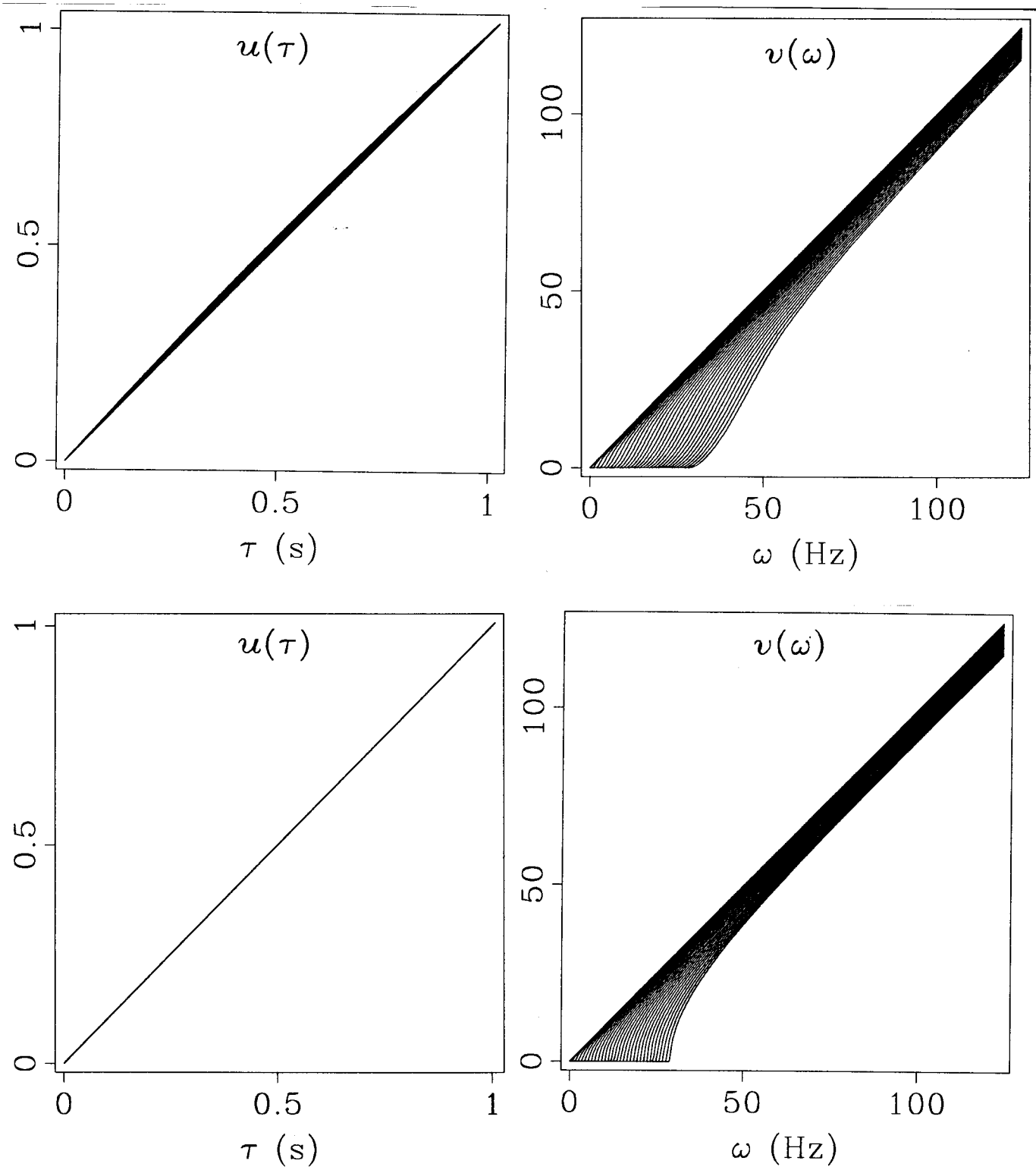

FIG. 1. SVD-Stolt mappings for a linear velocity function $1500 + 250t$ m/s (top) and a constant 1500 m/s (bottom). The τ mapping u is on the left; the ω mapping v is on the right. The main diagonals are the identity function we get for $k = 0$; the adjacent curves are for increasing values of k.

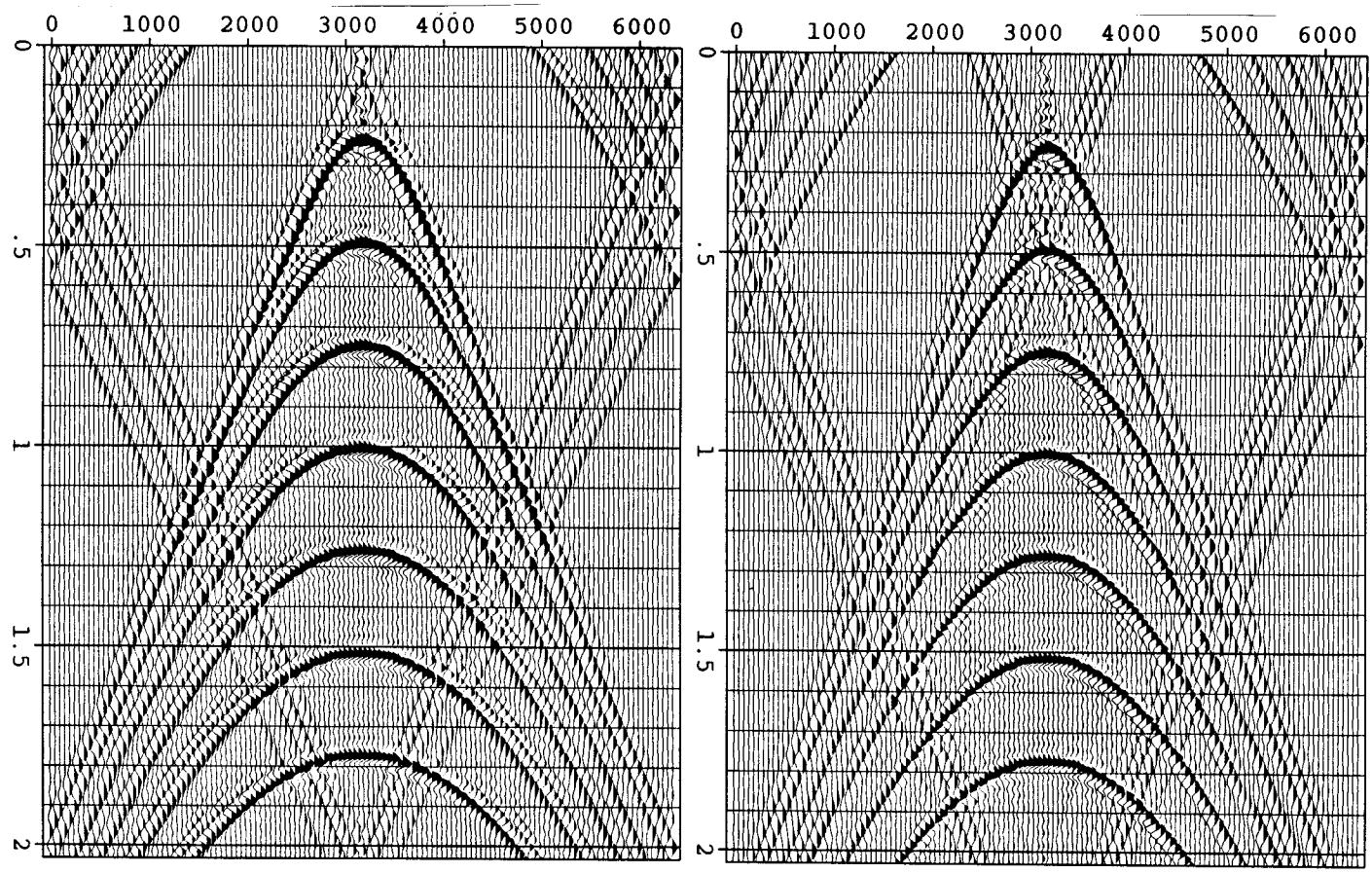

FIG. 2. SVD-Stolt modelling of 7 point scatterers. On the left is constant velocity modeling; on the right is modeling with a velocity of 1500 + 250 m/s. These correspond to the mapping functions displayed in Fig. 1. Trace spacing is 50 m; time sampling interval is 16 ms.

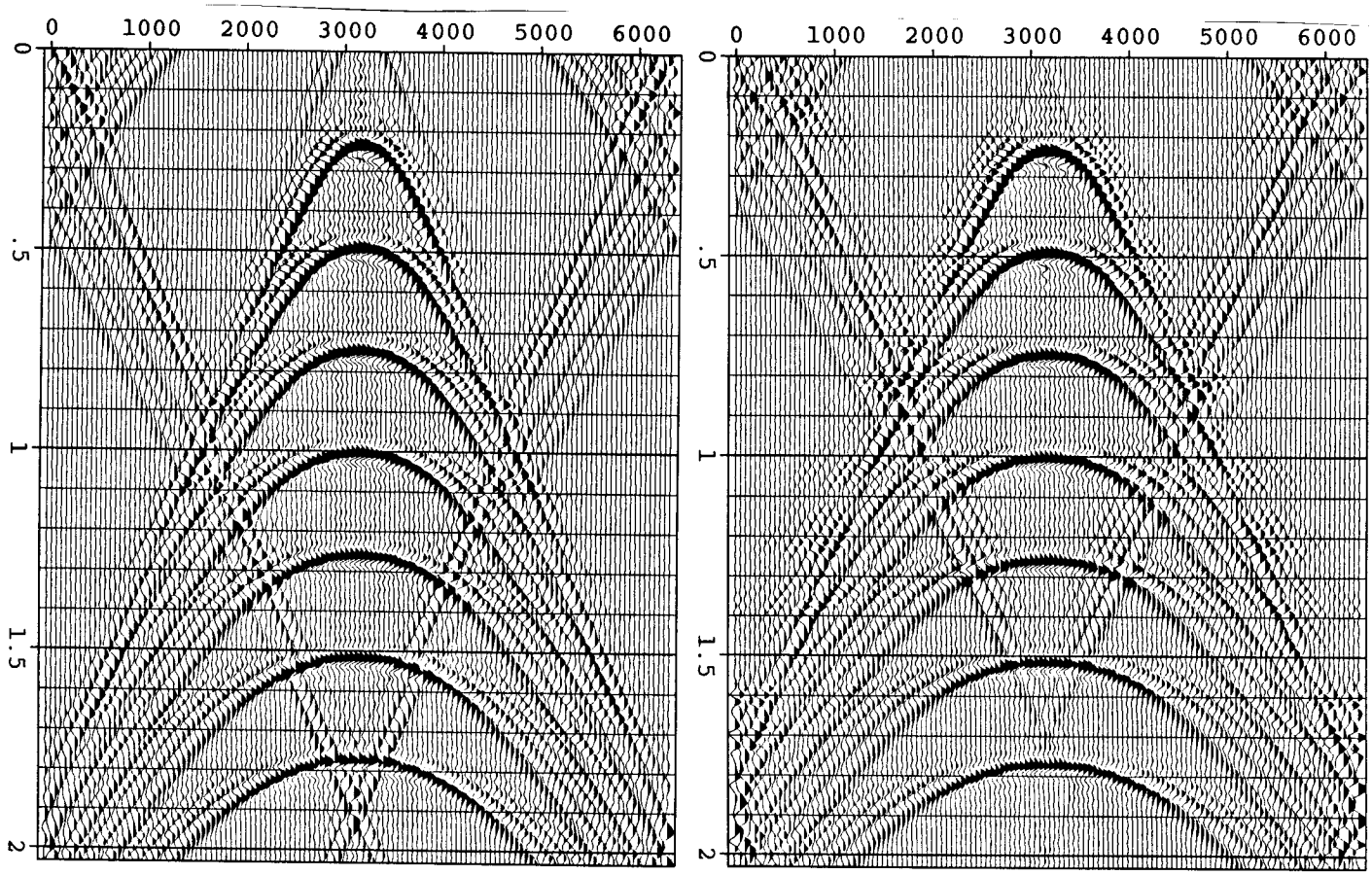

FIG. 3. SVD-Stolt modelling with larger velocity gradients. On the left the velocity function is $1500 + 500t$ m/s; on the right we use $1500 + 750t$. Dispersion increases beyond acceptable levels.

For computation, the complete singular value decomposition is extravagant. Simple iteration by the power method (Householder 1964, 187-190) or the Lanczos process (Golub and Van Loan 1983, Chap. 9) produces the largest singular value and corresponding singular vectors; the sum of squares of all the singular values is given by $\mathbf{tr}(\phi^T \phi)$. Also, convergence of the iterations is dominated by the geometric progression $|\lambda_1/\lambda_2|^i$ and thus will be extremely rapid if the fit is at all good.

SVD-STOLT MIGRATION

The SVD-Stolt method can most immediately be applied to migration of seismic data. Given a stratified interval velocity v(t), the aim here is to replace phase-shift migration using

$$\phi = \int_0^\tau \text{sgn}\ \omega \left(\omega^2 - v(t)^2 k^2\right)^{1/2} dt \tag{5}$$

with migration based upon the SVD-Stolt approximation. Since we have the perfect fit in equation (4) when velocity is constant, we have assurance that a good fit will be manifest for sufficiently small deviations from constant velocity.

Figure 1 displays the SVD-Stolt mapping functions for a linear velocity gradient $1500 + 250t$ m/s. These mapping functions were fit over the complete ω–k plane from DC to Nyquist. Fitting error was on the order of 1%. For reference, the curves for a constant 1500 m/s are also shown. Figure 2 shows SVD-Stolt modelling with those mapping functions. Measured velocities for the hyperbolas are within 5% of the RMS velocities predicted by the Dix formula. Again, the corresponding model for a constant 1500 m/s is shown for comparison.

We see that the SVD-Stolt migration has worked well for this gentle velocity gradient. Noticeable dispersion creeps in as the velocity gradient increases, as seen in Fig. 3 for gradients of 500 and 750 m/s. Here, the fitting error increases to about 5%. These results can surely be improved cosmetically with more careful crafting of the fitting functions. They show, however, the ranges of velocity variation and dip one can expect to handle with the SVD-Stolt method.

SVD-STOLT DIP MOVEOUT

A pure-phase approximation for dip moveout (DMO) may be obtained by Fourier-transforming the DMO impulse response and dividing each ω–k sample by its modulus. This impulse response could be computed exactly using wave theory (Deregowski and Rocca 1981; Hale 1983). For economy and simplicity, however, we will derive our approximation by traveltime arguments.

On a common-offset section with half-offset h, an impulse at $(x=0,\ t=t_h)$ corresponds to the zero offset ellipse

$$t_o^2 = t_h^2 \left(1 - \frac{x^2}{h^2}\right) \quad . \tag{6}$$

The impulse is a superposition of straight lines radiating in all directions from the point. The ellipse is a superposition of straight lines tangent to each of its individual points. To convert the impulse into the ellipse, we can vertically time shift each dipping line passing through the point so that it becomes tangent to the ellipse as illustrated in Figure 4.

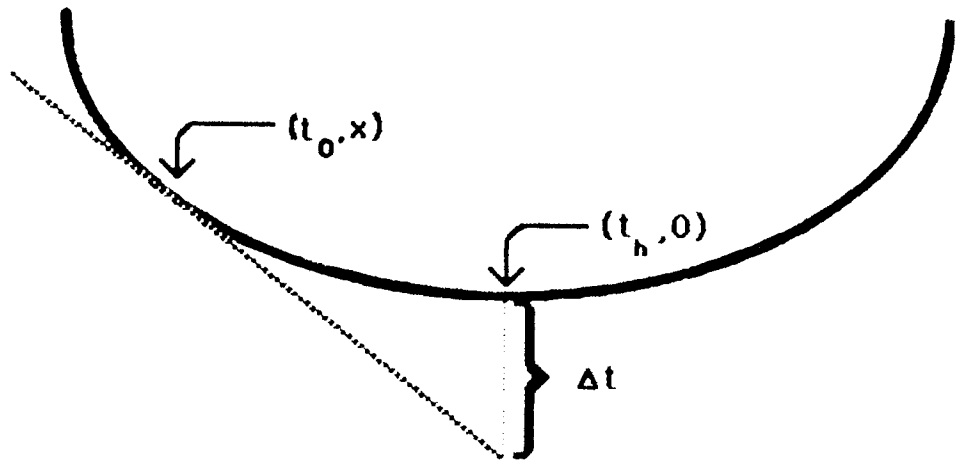

FIG. 4. Time shift Δt needed to collapse the DMO ellipse to an impulse at the point $(t_o\ , x=0)$. The corresponding phase shift is $\omega \Delta t$.

The slope $dt_o\,/dx$ of the tangent line becomes $k\,/\omega$ after Fourier transform to the $k-\omega$ domain. The phase shift corresponding to shifting the tangent by Δt is $\omega \Delta t$. The total phase shift ϕ in equation (1) is $\omega t_h + \omega \Delta t$. Since Δt is given by $t_o + x\ dt_o\,/dx - t_h$, the total phase shift is then $\omega t_o + kx$.

To evaluate $\omega t_o + kx$ in terms of t_h , k , and ω, we can differentiate equation (6) to find

$$\frac{k}{\omega} = \frac{dt_o}{dx} = -\frac{x t_h{}^2}{t_o\, h^2} \quad . \tag{7}$$

Solving this for x yields

$$x = h\Big(1 + (\omega t_h\,/kh\,)^2\Big)^{-1/2} \quad . \tag{8}$$

With this solution for x , we substitute into equation (6) to get

$$t_o = t_h\,(\omega t_h\,/kh\,)\Big(1 + (\omega t_h\,/kh\,)^2\Big)^{-1/2} \quad . \tag{9}$$

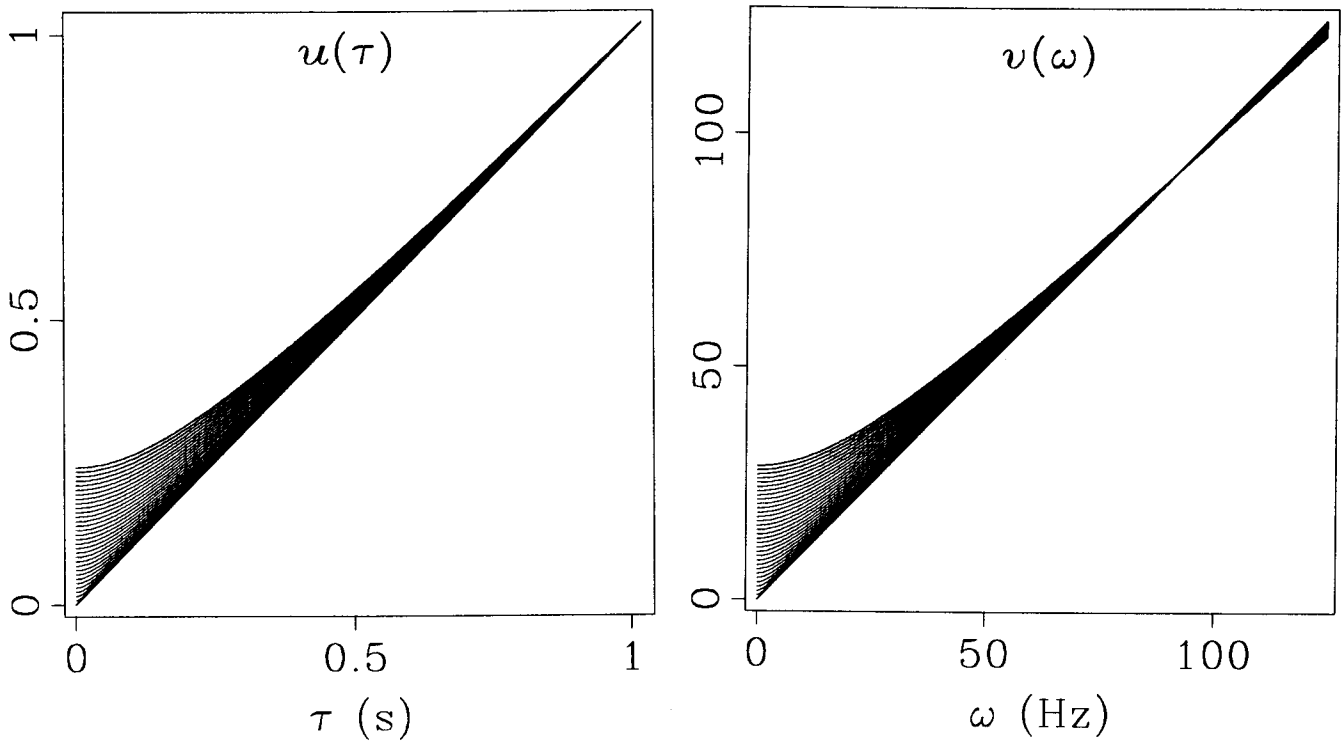

FIG. 5. SVD-Stolt mapping functions for dip moveout. On the left is the τ map; on the right the ω map. Again, we see the curves for increasing k moving away from the diagonal. The shapes are not identical because we have restricted our fitting domain to τ greater than a mute time τ_0 to avoid the DMO singularity at τ=0.

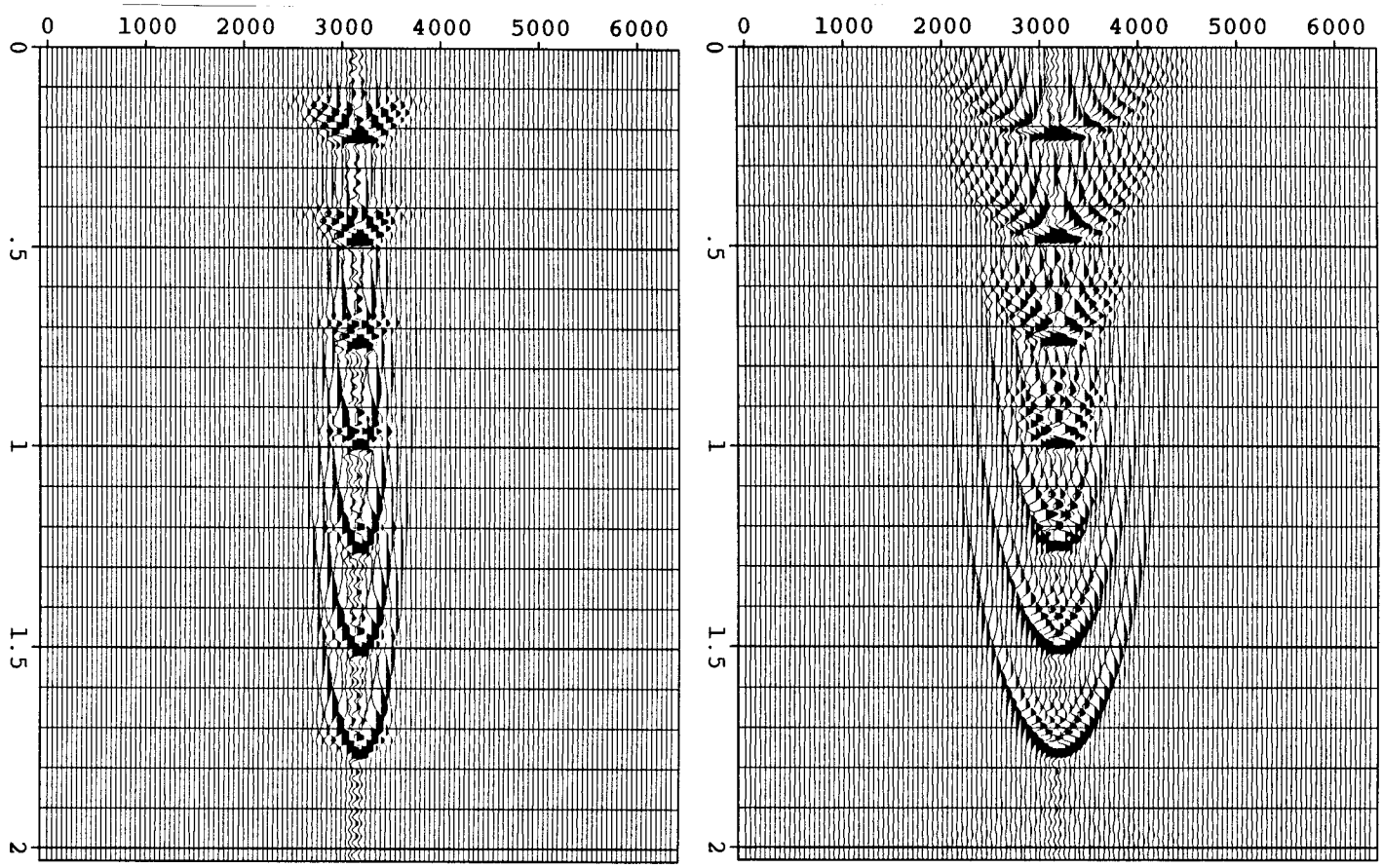

FIG. 6. SVD-Stolt modelling of the DMO ellipse at nonzero offset. Here the half-offsets are 500 and 1000 m for the left and right respectively. Trace spacing is 50 m; time sampling interval is 16 ms. A breakdown at shallow times and long offsets is evident.

After simplification, we arrive at the total phase shift

$$\phi \;=\; \omega t_o \;+\; kx \;\;=\;\; \left(\omega^2 {t_h}^2 + k^2 h^2\right)^{1/2} \quad . \tag{10}$$

Here, t_h is the equivalent to τ.

In Figure 5, we show mapping functions fit to the DMO phase of equation (10). These curves resemble the inverse mappings the migration curves of Fig. 1. This reflects the anti-migration of DMO in collapsing the elliptical smile in Fig. 4 to a point. Figure 6 is the dip-moveout smile modelled with the SVD-Stolt method for half-offsets of 500 and 1000 m. These results are too dispersive at shallow times.

FURTHER APPLICATIONS

For migration of stacked sections, SVD-Stolt migration is most useful for smooth, gently sloping velocity functions. In that case the phase shifts ϕ are also smooth and only a coarse sampling is needed to compute a good separable approximation. This is critical, as obtaining the separable SVD approximation involves some matrix multiplications with the phase shifts. One might just as well apply the phase shifts directly if they had to be sampled finely.

SVD-Stolt migration with short, linear velocity ramps can also be used as an interpolator between depth levels in phase-shift migration to maintain accuracy while saving computer time by using large depth extrapolation steps. In this setting, it's possible to pretabulate or analytically approximate the needed Stolt mapping functions.

Prestack and 3-D migration offer more latitude for using SVD-Stolt migration. Here we have redundancy – many gathers or planes can be migrated with the same mapping functions. Only one phase shift SVD decomposition is needed at the start of the computation.

For velocity independent dip moveout, there are already other methods that run at FFT speeds, such as the shot-profile method of Biondo and Ronen (1986). These use a logarithmic stretch of the time axis to make the dip-moveout operator a time-invariant convolution. SVD-Stolt DMO uses the same number of stretch operations, but interpolates complex numbers instead of real numbers; it is likely to run somewhat slower as a result, though possibly with different artifacts.

For velocity-dependent dip moveout the SVD-Stolt method offers a reasonable way to handle velocity corrections. The phase surface can be sketched out by tracing a few rays, adding a reasonably small amount to the overall computation. This extension is contingent upon improving the quality of our velocity-independent SVD-Stolt DMO.

DIRECTIONS FOR RESEARCH

Stolt mapping vs. Stolt stretch

Stolt (1978) adapts his constant velocity migration to variable velocity by different means. The original traces are first stretched with a function that makes all migration hyperbolas appear to have the same velocity near their apices (Levin 1983;1985b). The stretched section is then Fourier transformed and mapped with a modified dispersion relation that partially adjusts for the generally higher apparent velocity associated with wide-angle arrivals (Levin 1985b; Sword 1987). After inverse transforms, the resulting traces are then unstretched to for the final image.

Our SVD-Stolt migration replaces only Stolt's mapping function. We are still able to use trace stretching to augment the process. The purpose would be to increase the separation of the largest singular value of our phase decomposition from the remaining singular values. This would increase the accuracy of the separable fit, yielding greater migration accuracy. As yet, we do not have machinery that creates analogues to Stolt stretch. How to generate Stolt stretch or the DMO log stretch without case-by-case analysis and experimentation remains a mystery.

Divide and conquer

In our examples, we have computed one SVD decomposition to apply to the full dataset. For better accuracy, we could divide the ω–k plane (or the τ–k plane) into smaller pieces. Each piece would then be processed individually with a different separable fit. With dip decomposition, i.e. pie-slice filters, we obtain a method along the lines suggested in Levin (1984) for extending the domain of ordinary Stolt migration. This does not necessarily increase the cost of the migration greatly. The frequency mapping $v(\omega)$ is now restricted to only subsets of the ω axis, leading to economies in both the mapping and the inverse Fourier transform.

Amplitude

Pure-phase processing has been our focus in this paper. The only amplitudes corrections we have applied have been the Jacobians of the SVD mappings. Dip moveout is not really a pure-phase partial migration. It has amplitude corrections that we have ignored in our traveltime development. Separable approximation of these amplitude factors is also possible; these can be applied simultaneously with the u and v change of variable.

CONCLUSIONS

We have presented a new method that permits fast computational approximations for quite general phase-shift imaging problems. This method uses singular value decomposition to generalize Stolt's Fourier migration method. Separable approximation of the phase shifts produces a change of variable that turns the computation into a Fourier transform, one rapidly performed with FFT methods. The Stolt-SVD method has been applied both to phase-shift migration with a vertically-varying velocity function and to dip moveout correction of common-offset data. We have indicated additional uses for the method and directions for further research and development.

REFERENCES

Deregowski, S.M. and Rocca, F., 1981, Geometrical optics and wave theory of constant-offset sections in layered media: Geoph. Prosp., 29, 384-406.

Golub, G.H. and Van Loan, C.F., 1983, Matrix computations: Johns Hopkins Univ. Press.

Hale, D., 1984, Dip moveout by Fourier transform: Geophysics, 49, 741-757.

Householder, A.S., 1964, The theory of matrices in numerical analysis: Blaisdell Publ. Co., reprinted 1975 by Dover Publ.

Levin, S.A., 1983, Remarks on two-pass 3-D migration error: SEP-35, 195-200.

Levin, S.A., 1984, An analysis of p-Stolt stretch: SEP-38, 165-170.

Levin, S.A., 1985a, Newton trace balancing: SEP-42, 69-80.

Levin, S.A., 1985b, Understanding Stolt stretch: SEP-42, 373-374.

Stolt, R.H., 1978, Migration by Fourier transform: Geophysics 43, 23-48.

Sword, C., 1987, A Soviet look at datum shift: SEP-51, 313-316.